J integral strain-curvature approach for multilayer fracture specimens with unknown thickness and stiffness of layers

Sørensen, B. F.; Toftegaard, H. L.

Published in:
43rd Risoe International Symposium on Materials Science

Link to article, DOI:
10.1088/1757-899X/1293/1/012024

Publication date:
2023

Document Version
Publisher's PDF, also known as Version of record

J integral strain-curvature approach for multilayer fracture specimens with unknown thickness and stiffness of layers

J integral strain-curvature approach for multilayer fracture specimens with unknown thickness and stiffness of layers

B F Sørensen[1] **and H L Toftegaard**[1]

[1]Technical University of Denmark, DTU Wind and Energy Systems, Risø Campus Frederiksborgvej 399, DK-4000 Roskilde, Denmark

E-mail: bsqr@dtu.dk

Abstract. In the coming years, many wind turbines will reach their planned design life, and it is of great interest to investigate if their service life can be extended so that the turbines can produce a larger amount of electricity before decommissioning. Such an assessment can include the measurement of the fracture mechanics properties of materials interfaces, e.g., for trailing edge bondlines, web foot bondlines and interfaces between layers in the load-carrying main spars. It would then be preferable to conduct the fracture mechanics testing and data analysis by approaches that give accurate results with the smallest amount of testing. In the present work we propose an approach for measurement of mixed mode fracture resistance (and mixed cohesive laws) that does not require knowledge of the stiffness properties and the elastic centre of the laminates of the test specimens. This is advantageous since the layer stiffness, layer thickness and the lay-up of a laminate cut from an old blade may not be known. Furthermore, the elastic properties of polymer resins of bondlines and matrix materials in fibre composites can have changed (aging) due to the blades long-time environmental exposure.

1. Introduction

When the use-time of a wind turbine in a wind farm is close to the projected service life (typically, 20 to 25 years), it is relevant to consider if the service life of the turbines can be extended in order to get more energy produced before the turbine is taken out of service. The process of assessing the extension of the use-life of old wind turbine rotor blades in a wind turbine park can involve the characterization of the mechanical properties of the materials and interfaces by testing specimens cut from a single representative blade. The fracture mechanics properties of the blade can then be used to assess the growth of damages in the blades of the remaining turbines. The primary load-carrying parts of a wind turbine blade is made of layers of composites materials (typically, made of glass and/or carbon fibres in a polymer matrix) and therefore it would be relevant to make fracture mechanics testing of interfaces between layers in laminates (e.g., within the main spar) and laminate/adhesive interfaces (e.g., web-foot and trailing edge bondlines). It would be convenient to cut fracture mechanics specimens of regular shape from a blade, so that established fracture mechanics testing procedures can be used. There are well-established fracture mechanics testing methods for linear elastic fracture mechanics characterisation, both for pure Mode I and mixed mode [1, 2] (valid for small scale fracture process zone) and J integral test specimens (valid for both small-scale fracture process zones and large scale bridging problems) [3, 4].

However, the elastic properties, thickness and orientation of each layer may not be known for fracture mechanics test specimens cut from an old wind turbine blades. Therefore, it would be convenient to use fracture mechanics testing methods for which the calculation of the fracture mechanics properties (mixed mode fracture resistance or mixed mode cohesive laws) can be done without the need for knowing the elastic properties and thickness of the individual layers. For Mode I Double Cantilever Beam (DCB) specimens loaded with wedge forces or bending moments, there are known J integral equations that are independent of the elastic properties [5, 6, 7]. These approaches have been generalized

to DCB specimen mixed mode specimens loaded by transverse forces [8] and DCB specimen loaded with axial forces and bending moments [9]. For beam-like specimens loaded by axial forces and bending moments the J integral solution can be expressed in terms of the applied axial forces, bending moments as well as the curvature and the axial strain of the elastic centres of the specimen beams [9]. Neither the elastic properties of the individual layers nor the elastic properties of the beams are required. The approach is fairly general; it is applicable for multilayered and graded specimens and, as a J integral solution, remains valid for both small scale fracture (linear elastic fracture mechanics conditions) and for large-scale bridging problems. The approach requires, however, knowledge of the elastic centres for each of the three beams of the DCB-specimen. Although this can be determined experimentally [9], it would be preferable if these additional measurements were not required. Only in the absence of axial forces (i.e., pure bending), the approach does not require knowledge of the elastic centre.

The purpose of the present paper is to establish a J integral equation where forces, moments, curvatures and axial strains are defined from the geometric mid-plane instead of the elastic centre. It is found that while the bending moments and axial strains are different from those defined from the elastic centres, the J integral equation takes the exact same mathematical form. This enables a novel fracture mechanics testing approach, which only requires the overall dimensions (thickness and width) of each beam as well as continuous measurements of the applied axial forces, moments, curvatures and axial strains of the geometric mid-plane of each beam. The strains and curvatures can be measured experimentally by the use of the digital image correlation technique, e.g. by measurement of axial strains at the top and bottom of the three beams, i.e. six strain measurements. For the measurement of the fracture resistance to be accurate, it is necessary that these strains are measured with sufficient accuracy. It is therefore also important to consider how these strains can be measured. Strain gauges are known to be very accurate but could be difficult to place on beams running parallel to each other. Therefore, the use of digital image correlation (DIC) [10] should be considered. However, since strain measurements by DIC are not as accurate as strain measurements by strain gauges, this paper considers how to check, if the accuracy is sufficient to enable J integral measurement from curvature measurements obtained from DIC.

The paper is organised as follows. First, in Section 2 we define the problem. In Section 3, we prove mathematically that the J equation of Toftegaard and Sørensen [9] holds true irrespective of what coordinate system is used to define forces and moments, and set up equations for estimation of the uncertainty of the J integral value accounting for uncertainties associated with DIC strain measurements. Section 4 presents results in the form of tables for the estimated uncertainties. Section 5 discusses the advantages and disadvantages of the proposed approach, and Section 6 contains the main conclusion of the study.

2. Problem description

The problem we consider is a beam-like fracture specimen consisting of three beams, as shown in figure 1. The specimen has a constant width, B and the beam height is denoted H_1, H_2 and H_3, for Beam 1, Beam 2 and Beam 3, respectively. The specimen can consist of a single, homogenous, linear-elastic material or of multiple layers made of orthotropic materials oriented parallel to the plane of the fracture process zone (the x_1-x_3-plane) or the elastic properties can be graded in the x_2-direction, but must be independent of the x_1-position. For a layered structure, the elastic properties and the layer thicknesses must be independent of the x_1-coordinate. The specimen is loaded with a combination of axial forces and bending moments. The axial forces, acting at the elastic centres, are denoted by N_1, N_2 and N_3 (subscript indicates beam number), and the bending moments are denoted M_1, M_2 and M_3. The forces and moments are taken to be positive as indicated in figure 1. The distance from the ends (where the forces and moments apply) to the fracture process zone is several times the beam thickness. The fracture process zone may not necessary be small, it can include large-scale fibre bridging. Therefore, we will analyse the specimen by the path-independent J integral [11], not by linear elastic fracture mechanics.

As mentioned above, this problem has been analysed by Toftegaard and Sørensen [9]. The J integral evaluation around the external boundaries can be written as

$$J_{ext} = \frac{N_1\varepsilon_1^0}{2B} + \frac{N_2\varepsilon_2^0}{2B} - \frac{N_3\varepsilon_3^0}{2B} + \frac{M_1\kappa_1}{2B} + \frac{M_2\kappa_2}{2B} - \frac{M_3\kappa_3}{2B}, \quad (1)$$

where ε_1^0, ε_2^0 and ε_3^0 are the axial strain component, ε_{11}, at the elastic centres of Beam 1, Beam 2 and Beam 3, and κ_1, κ_2 and κ_3 are the (elastic centre axis) curvatures of Beam 1, Beam 2 and Beam 3. Thus, by measuring the strain at the elastic centres and the curvatures along with the applied axial forces and moments, the J integral value can be determined without needing to know anything about the elastic properties of the beams, except that they are linearly elastic.

But this approach requires the knowledge of the position of the elastic centre for each of the three beams. In the following, we will express (1) in terms of axial forces and moments associated with the geometric mid-height of each beam instead of the elastic centre of each beam.

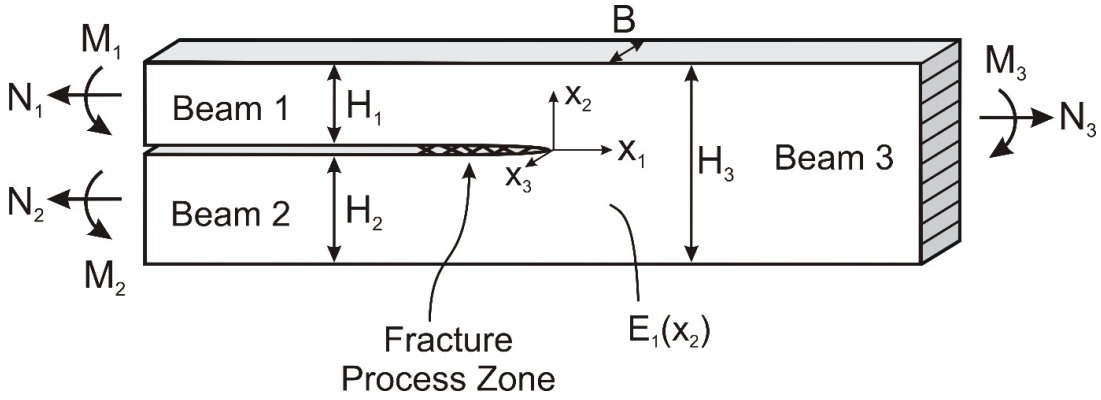

Figure 1. The problem under investigation: A beam-like specimen loaded with axial forces and bending moments remote from the fracture process zone. The elastic properties of the beams are independent of the x_1 coordinate but can vary layer wise or graded in the x_2-direction.

3. Mathematical derivation

3.1. J integral result

In the following, we will analyse the J integral contribution from Beam 2 with reference to two coordinate systems, one located at the elastic centre and another coordinate system located elsewhere (e.g., at the geometric mid-height), as shown in figure 2. The J integral is evaluated away from the fracture process zone, where the stress and strain fields are uniform, i.e., independent of the x_1-position [9]. Define the local coordinate system with origin in the elastic centre by $(\bar{x}_2, \bar{y}_2, \bar{z}_2)$, and the other coordinate system by (x_2^*, y_2^*, z_2^*) (for both coordinate systems, subscript 2 indicates Beam 2). In the global x_i-coordinate system, the x_2-coordinate of the elastic centre is denoted by δ_2 and the x_2-coordinate of the origin of the other coordinate system is denoted ξ_2 (again, for both symbols, subscript 2 is used to denote Beam 2). The axial force and moment defined with reference to the (x_2^*, y_2^*, z_2^*)-coordinate system is denoted N_2^* and M_2^*.

From (1) it follows that the J integral contribution for an integration path from top to bottom of Beam 2 is (subscript 2 is used to indicate Beam 2)

$$J_2 = \frac{N_2\varepsilon_2^0}{2B} + \frac{M_2\kappa_2}{2B}. \quad (2)$$

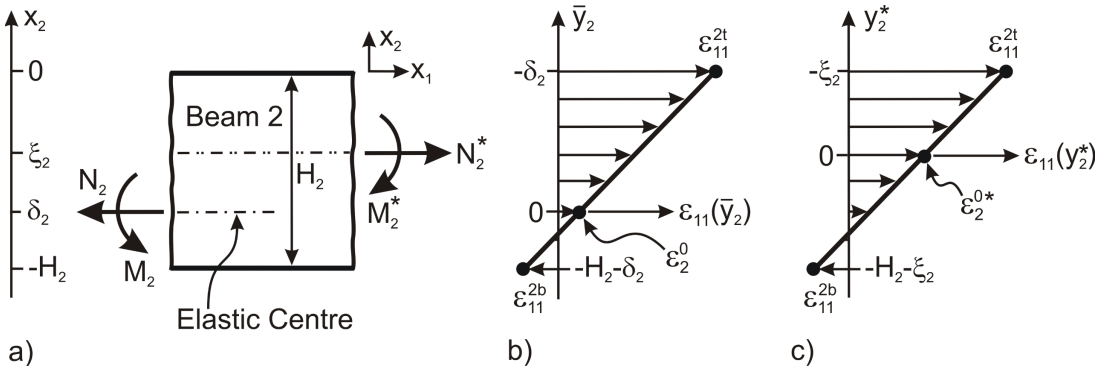

Figure 2. The definition of the axial force, moment, strain and curvature with respect to the two coordinate axes, $\bar{y}_2$, and y_2^*.

With respect to the original $\bar{y}_2$-coordinate, the normal strain in Beam 2 can be written as

$$\varepsilon_{11}(\bar{y}_2) = \varepsilon_2^0 + \kappa_2 \bar{y}_2 \,, \tag{3}$$

where $\varepsilon_2^0 = \varepsilon_{11}(x_2 = \delta_2)$. In the (x_2^*, y_2^*, z_2^*)-coordinate system the strain distribution would be written as

$$\varepsilon_{11}(y_2^*) = \varepsilon_2^{0*} + \kappa_2 y_2^* \,, \tag{4}$$

where $\varepsilon_2^{0*} = \varepsilon_{11}(x_2 = \xi_2)$. Note that the curvature κ_2 is the same for both descriptions. Since $x_2 = \delta_2 + \bar{y}_2 = \xi_2 + y_2^*$, the relation between $\bar{y}_2$ and y_2^* is

$$\bar{y}_2 = y_2^* + \xi_2 - \delta_2. \tag{5}$$

We proceed by expressing ε_2^0 in terms of ε_2^{0*}. By setting $y_2^* = 0$ (and thus by (5), $\bar{y}_2 = \xi_2 - \delta_2$), we get from (3) and (4) using (5):

$$\varepsilon_2^0 = \varepsilon_2^{0*} - \kappa_2(\xi_2 - \delta_2). \tag{6}$$

Next, from force equilibrium we find:

$$N_2 = N_2^* \qquad and \qquad M_2 = M_2^* + N_2^*(\xi_2 - \delta_2) \,. \tag{7}$$

Finally, we insert N_2 from (7), ε_2^0 from (6) and M_2 from (7) into (2):

$$J_2 = \frac{N_2^*}{2B}[\varepsilon_2^{0*} - \kappa_2(\xi_2 - \delta_2)] + \frac{\kappa_2}{2B}[M_2^* + N_2^*(\xi_2 - \delta_2)] \,, \tag{8}$$

and tidying up we notice that the terms with ξ_2 and δ_2 cancel out, so that eq. (8) reduces to

$$J_2 = \frac{N_2^* \varepsilon_2^{0*}}{2B} + \frac{M_2^* \kappa_2}{2B}. \tag{9}$$

The J integral equation expressed in the (x_2^*, y_2^*, z_2^*)-coordinate system, eq. (9), takes exactly the *same mathematical form* as the J integral expression with the normal force and moment defined from the elastic centre, eq. (2), with N_2 replaced by N_2^*, ε_2^0 replaced by ε_2^{0*} and M_2 replaced by M_2^*. It follows, that we do not need to define the axial force and moment from the elastic centre of the beam. Irrespective of what coordinate system is used when defining the axial force and moment, the same J integral equation applies.

Similar results can be found for Beam 1 and Beam 3 (since the integration path of Beam 3 is opposite of the integration path of Beam 1 and Beam 2, the J integral contributions become negative), so that the J integral evaluated around the external boundaries of the specimen can be written as

$$J_{ext} = \frac{N_1^* \varepsilon_1^{0*}}{2B} + \frac{M_1^* \kappa_1}{2B} + \frac{N_2^* \varepsilon_2^{0*}}{2B} + \frac{M_2^* \kappa_2}{2B} - \frac{N_3^* \varepsilon_3^{0*}}{2B} + \frac{M_3^* \kappa_3}{2B}. \quad (10)$$

where N_1^* and M_1^* and N_3^* and M_3^* are the axial force and moments applied to Beam 1 and Beam 3, respectively, being defined from conveniently chosen local (x_1^*, y_1^*, z_1^*)- and (x_3^*, y_3^*, z_3^*)-coordinate systems for the two beams. Eq. (10) is our main result.

3.2. Measurements of ε_2^{0*} and κ_2 from surface strains

In practice, the variables ε_1^{0*}, κ_1, ε_2^{0*}, κ_2 as well as ε_3^{0*} and κ_3 must be measured during fracture experiments. Focussing again on Beam 2, we will now describe an approach from which we can determine ε_2^{0*} and κ_2 from measurements of the axial strain at the top and bottom of the beam. Denote the axial strain at the top of the beam by ε_{11}^{2t} and the axial strain at the bottom of the beam by ε_{11}^{2b} (see figure 2). From (4) we get the strains as:

$$\varepsilon_{11}^{2t} = \varepsilon_{11}(y_2^* = 0 - \xi_2) = \varepsilon_2^{0*} - \kappa_2 \xi_2 , \quad (11)$$

and

$$\varepsilon_{11}^{2b} = \varepsilon_{11}(y_2^* = -H_2 - \xi_2) = \varepsilon_2^{0*} - \kappa_2 (H_2 + \xi_2) . \quad (12)$$

Solving the two equations (11) and (12) for ε_2^{0*} and κ_2 gives

$$\varepsilon_2^{0*} = \varepsilon_{11}^{2t} \left(1 + \frac{\xi_2}{H_2}\right) - \varepsilon_{11}^{2b} \frac{\xi_2}{H_2} \quad (13)$$

and

$$\kappa_2 = \frac{\left(\varepsilon_{11}^{2t} - \varepsilon_{11}^{2b}\right)}{H_2}. \quad (14)$$

Note that (14) is independent of the choice of ξ_2.

For the special case that the coordinate system is chosen at the geometric mid-plane of the beam, $\xi_2 = -H_2/2$, eq. (13) reduces to the expected result

$$\varepsilon_2^{0*} = \frac{\left(\varepsilon_{11}^{2t} + \varepsilon_{11}^{2b}\right)}{2}. \quad (15)$$

Similar equations apply for Beam 1 and Beam 3, i.e., for ε_1^{0*}, κ_1, ε_3^{0*} and κ_3.

To sum up, the width B should be measured before the experiment, and the following variables should be measured during the experiment: N_1^*, M_1^*, ε_{11}^{1t}, ε_{11}^{1b} (Beam 1); N_2^*, M_2^*, ε_{11}^{2t}, ε_{11}^{2b} (Beam 2); N_3^*, M_3^*, ε_{11}^{3t}, ε_{11}^{3b} (Beam 3).

3.3. Equations for sensitivity analysis

Before using the proposed approach experimentally, it is useful to contemplate the accuracy of the approach of measuring axial strains and curvatures instead of measuring the extension and bending stiffness properties of the three beams, Beam 1, Beam 2 and Beam 3. In the following we will present some simple estimates of the uncertainties on the J integral contributions. Our focus will be on the sensitivity of the measurement of curvature from strain measurements in accordance with (14). For simplicity we will consider a symmetric (i.e., identical beam heights, $H_1 = H_2$), homogenous DCB-specimen loaded with symmetric moments, $M_1 = -M_2$ (with $M_2 > 0$), with $N_1 = N_2 = N_3 = 0$ and $M_3 = 0$. In an experiment, the relevant moments and strains (M_2, ε_{11}^{2t} and ε_{11}^{2b}) would be measured. In this sensitivity analysis we instead assume the material to have a certain stiffness (Young's modulus)

and set up some equations to establish consistent sets of moments and strains as a function of J_{ext} and H_2.

For a symmetric, homogenous DCB-specimen loaded with symmetric moments (Mode I), the J integral result (10) (or equivalently (1)) reduces to

$$J_{ext} = \frac{M_2 \kappa_2}{B}. \tag{16}$$

Assuming that Beam 1 and Beam 2 are homogeneous beams, it follows that $\xi_1 = \delta_1 = H_2/2$ and $\xi_2 = \delta_2 = -H_2/2$. With the moment of inertia of the rectangular cross section of Beam 1 and Beam 2 given by [12]

$$I = \frac{B(H_2)^3}{12}, \tag{17}$$

and the Young's modulus in the x_1-direction denoted by E_{11}, the moment is given by [12]

$$M_2 = E_{11} I \kappa_2 , \tag{18}$$

we find by inserting κ_2 (expressed in terms of M_2) from (18) into (16)

$$J_{ext} = \frac{(M_2)^2}{B E_{11} I}. \tag{19}$$

From (19), we can find the moment required for a given J integral value:

$$M_2 = \sqrt{J_{ext} B E_{11} I} . \tag{20}$$

Eq. (20) gives M_2 as a function of H_2 (since I depends on H_2, see (17)). With M_2 determined, we can derive equations for ε_{11}^{2t} and ε_{11}^{2b}. With $N_2 = 0$, ε_2^{0*} must be zero for a homogenous specimen. An equation for Beam 2, similar to (14), gives

$$\varepsilon_{11}^{2b} = -\varepsilon_{11}^{2t} , \tag{21}$$

so that an equation for Beam 2 similar to (15) gives

$$\kappa_2 = \frac{2\varepsilon_{11}^{2t}}{H_2} , \tag{22}$$

or

$$\varepsilon_{11}^{2t} = \frac{H_2 \kappa_2}{2}. \tag{23}$$

Now we can set up calculations to assess the uncertainly calculations. Since, in some test configurations, the bending moment is generated by a force couple [3], we will consider the uncertainty of the moment in terms of both the applied force, P, and the moment arm, ℓ_2, where the moment is given by

$$M_2 = P \ell_2 . \tag{24}$$

Then, by (22) and (24), the J integral equation (16) becomes (dropping the subscript of J_{ext})

$$J = \frac{2P\ell_2 \varepsilon_{11}^{2t}}{B H_2}. \tag{25}$$

The uncertainty of J, denoted by ΔJ, can now be estimated using the general formula for error propagation [13], as follows:

$$(\Delta J)^2 = \left(\frac{\partial J}{\partial P}\Delta P\right)^2 + \left(\frac{\partial J}{\partial \ell_2}\Delta \ell_2\right)^2 + \left(\frac{\partial J}{\partial B}\Delta B\right)^2 + \left(\frac{\partial J}{\partial H_2}\Delta H_2\right)^2 + \left(\frac{\partial J}{\partial \varepsilon_{11}^{2t}}\Delta \varepsilon_{11}^{2t}\right)^2, \quad (26)$$

where ΔP, $\Delta \ell_2$, ΔB, ΔH_2 and $\Delta \varepsilon_{11}^{2t}$ are the uncertain of measured values of the applied force, P, the moment arm, ℓ_2, the specimen width, B, the specimen height, H_2 and the strain at the top of the beam, ε_{11}^{2t} , respectively. Partial differentiation of (25) gives

$$\frac{\partial J}{\partial P} = \frac{J}{P}, \quad \frac{\partial J}{\partial \ell_2} = \frac{J}{\ell_2}, \quad \frac{\partial J}{\partial B} = -\frac{J}{B}, \quad \frac{\partial J}{\partial H_2} = -\frac{J}{H_2}, \quad \frac{\partial J}{\partial \varepsilon_{11}^{2t}} = \frac{J}{\varepsilon_{11}^{2t}}. \quad (27)$$

Inserting (27) into (26) gives:

$$\left(\frac{\Delta J}{J}\right)^2 = \left(\frac{\Delta P}{P}\right)^2 + \left(\frac{\Delta \ell_2}{\ell_2}\right)^2 + \left(-\frac{\Delta B}{B}\right)^2 + \left(-\frac{\Delta H_2}{H_2}\right)^2 + \left(\frac{\Delta \varepsilon_{11}^{2t}}{\varepsilon_{11}^{2t}}\right)^2. \quad (28)$$

Taking the square root of (28) gives the relative uncertainty of J, $\Delta J/J$.

4. Results

4.1 Input parameters for sensitivity study

Although our analysis, Eq. (28), includes the sensitivity of all parameters, we will in the following focus on the effect of strain accuracy for curvature measurements. This is motivated by the fact that different strain measurement techniques have different accuracy, and it is important to choose ~~a~~ strain measurement techniques that lead to a sufficient accuracy result for the J integral value.

The uncertainty of strain measurements by foil strain gauges bonded to the surface is estimated to be ± 5 μstrain by Carlsson *et al*. [14]. Hannah and Reed [15] discuss many of the parameters that can influence the output from strain gauge measurement but wrote that, with reasonably care, one can realize strain readings accurate to ±2 % with a threshold strain sensitivity of 5 μstrain. Similar values can be found in other text books on strain measurements [16].

The uncertainty of strain measurements by DIC has been estimated to be about 10^{-4} (100 μstrain) [17]. In cases where the strain is uniform, the strain values for 100 images can be averaged and accuracy of the averaged value can be about 3 x 10^{-6} (3 μstrain) [18]. However, Reu *et al*. [19] found, comparing results from 11 different DIC codes, that for a varying strain field (Sample 14 in that study) that by averaging 50 rows of data, the standard deviation in the strain was between 172 x 10^{-6} to 875 x 10^{-6} (172 - 875 μstrain), with the majority in the range of 300 - 600 x 10^{-6} (300 - 600 μstrain).

In the following, we use these values of typical DCB test specimens for glass fibre composites: B = 30.0 mm, H_2 in the range of 2 to 16 mm and E_{11} = 40 GPa [4]. We use a moment arm with ℓ_2 = 86.5 mm. We investigate the situation of characterising a rather weak interface (fracture energy of 10 J/m^2), as well as a value corresponding to onset of crack growth of typical glass fibre composites (200 J/m^2) and a relative high fully-developed (steady-state) fracture resistance value (1000 J/m^2) [4].

We assume the following uncertainties: For the geometric dimensions we assume some uncertainties in measurement, ΔB = 0.1 mm, ΔH_2 = 0.2 mm and $\Delta \ell_2$ = 0.3 mm, while for the load, we take a load cell to be accurate within one percentage (twice the value claimed by a load-cell manufacturer [20]), thus we set $\Delta P/P$ = 0.01. Furthermore, with B and ℓ_2 fixed, we have $\Delta B/B$ = 3.33 x 10^{-3} and $\Delta \ell_2/\ell_2$ = 3.47 x 10^{-3}. For the strain measurement, we explore four values: A relative uncertainty of 2%, corresponding to the order of magnitude of uncertainty of strain gauges [15], uncertainties of 100 x 10^{-6} (100 μstrain), 300 x 10^{-6} (300 μstrain), and 600 x 10^{-6} (600 μstrain), the two last values taken to be representative of DIC [19].

Table 1 lists the squared uncertainty terms that are kept fixed in the present study. They constitute some of the parameter to go into (28). The remaining terms are explored next.

Table 1. Fixed uncertainty terms.

$\left(\frac{\Delta P}{P}\right)^2$	$\left(\frac{\Delta \ell_2}{\ell_2}\right)^2$	$\left(-\frac{\Delta B}{B}\right)^2$
100 x 10^{-6}	12 x 10^{-6}	11 x 10^{-6}

Specifying the fracture resistance, and thus the applied J integral value, J_{ext}, the stiffness, E_{11}, as well as the width and height of the beams, B and H_2, eq. (20) then gives the required moment, M_2. Next, κ_2 is calculated from (18), and from (23) we get ε_{11}^{2t}. Inserting these values together with the estimated uncertainty terms into (28) gives the relative uncertainty of J.

4.2. Estimated uncertainties

Results for uncertainty terms are shown in Table 2 for H_2 = 2 mm (rather thin DCB specimens for wind turbine blade materials [4]), Table 3 for H_2 = 8 mm (a representative DCB test height [4]) and Table 4 for H_2 = 16 mm (thicker specimens). The squared terms shown under the light green background colour enter eq. (28).

Table 2. Estimated uncertainty terms for beam height H_2= 2 mm calculated as a function of applied J value and various uncertainties of strain measurements. The strain uncertainty values in the fourth column from the left are absolute values ($\Delta\varepsilon_{11}^{2t}$) except for relative values ($\Delta\varepsilon_{11}^{2t}/\varepsilon_{11}^{2t}$) marked with #.

J (J/m^2)	P (N)	κ_2 (mm^{-1})	$\Delta\varepsilon_{11}^{2t}$ (-)	$\left(-\frac{\Delta H_2}{H_2}\right)^2$	$\left(\frac{\Delta\varepsilon_{11}^{2t}}{\varepsilon_{11}^{2t}}\right)^2$	$\left(\frac{\Delta J}{J}\right)$
10	5.66	0.612 x 10^{-3}	0.02$^{\#}$	0.01	0.40 x 10^{-3}	0.10
10	5.66	0.612 x 10^{-3}	100 x 10^{-6}	0.01	27 x 10^{-3}	0.19
10	5.66	0.612 x 10^{-3}	300 x 10^{-6}	0.01	0.24	0.50
10	5.66	0.612 x 10^{-3}	600 x 10^{-6}	0.01	0.96	0.98
200	25.3	2.74 x 10^{-3}	0.02$^{\#}$	0.01	0.40 x 10^{-3}	0.10
200	25.3	2.74 x 10^{-3}	100 x 10^{-6}	0.01	1.3 x 10^{-3}	0.11
200	25.3	2.74 x 10^{-3}	300 x 10^{-6}	0.01	12 x 10^{-3}	0.15
200	25.3	2.74 x 10^{-3}	600 x 10^{-6}	0.01	48 x 10^{-3}	0.24
1000	56.6	6.12 x 10^{-3}	0.02$^{\#}$	0.01	0.40 x 10^{-3}	0.10
1000	56.6	6.12 x 10^{-3}	100 x 10^{-6}	0.01	0.27 x 10^{-3}	0.10
1000	56.6	6.12 x 10^{-3}	300 x 10^{-6}	0.01	2.4 x 10^{-3}	0.11
1000	56.6	6.12 x 10^{-3}	600 x 10^{-6}	0.01	9.6 x 10^{-3}	0.14

Several points are noteworthy. Since it is not uncommon to experience a scatter of ±20% in fracture experiments [21], we choose an acceptance criterion of maximum 20% relative uncertainty on J (but other acceptance levels could also be argued). Then from Table 2 (H_2 = 2 mm) it is seen that for J = 10 J/m^2, a strain resolution of 100 μstrain is required. The expected resolution of DIC (300 μstrain) leads to an uncertainty of 50% in J, which, with the chosen acceptance criterion, would be unacceptable high for H_2 = 2 mm. Consulting Table 3 and Table 4, we note that an increasing value of H_2 (with all other parameters fixed) would result in an even higher uncertainty in in J.

Table 3. Estimated uncertainty terms for beam height H_2= 8 mm calculated as a function of applied J value and various uncertainties of strain measurements. The strain uncertainty values in the fourth column from the left are absolute values ($\Delta\varepsilon_{11}^{2t}$) except for relative values ($\Delta\varepsilon_{11}^{2t}/\varepsilon_{11}^{2t}$) marked with #.

J (J/m^2)	P (N)	κ_2 (mm^{-1})	$\Delta\varepsilon_{11}^{2t}$ (-)	$\left(-\frac{\Delta H_2}{H_2}\right)^2$	$\left(\frac{\Delta\varepsilon_{11}^{2t}}{\varepsilon_{11}^{2t}}\right)^2$	$\left(\frac{\Delta J}{J}\right)$
10	45.31	76.5 x 10^{-6}	0.02$^{\#}$	0.63 x 10^{-3}	0.4 x 10^{-3}	0.03
10	45.31	76.5 x 10^{-6}	100 x 10^{-6}	0.63 x 10^{-3}	0.11	0.33
10	45.31	76.5 x 10^{-6}	300 x 10^{-6}	0.63 x 10^{-3}	0.96	0.98
10	45.31	76.5 x 10^{-6}	600 x 10^{-6}	0.63 x 10^{-3}	3.8	1.96
200	202.6	0.342 x 10^{-3}	0.02$^{\#}$	0.63 x 10^{-3}	0.4 x 10^{-3}	0.03
200	202.6	0.342 x 10^{-3}	100 x 10^{-6}	0.63 x 10^{-3}	5.3 x 10^{-3}	0.08
200	202.6	0.342 x 10^{-3}	300 x 10^{-6}	0.63 x 10^{-3}	48 x 10^{-3}	0.22
200	202.6	0.342 x 10^{-3}	600 x 10^{-6}	0.63 x 10^{-3}	0.19	0.44
1000	453.1	0.765 x 10^{-3}	0.02$^{\#}$	0.63 x 10^{-3}	0.4 x 10^{-3}	0.03
1000	453.1	0.765 x 10^{-3}	100 x 10^{-6}	0.63 x 10^{-3}	1.1 x 10^{-3}	0.04
1000	453.1	0.765 x 10^{-3}	300 x 10^{-6}	0.63 x 10^{-3}	9.6 x 10^{-3}	0.10
1000	453.1	0.765 x 10^{-3}	600 x 10^{-6}	0.63 x 10^{-3}	38 x 10^{-3}	0.20

Table 4. Estimated uncertainty terms for beam height H_2= 16 mm calculated as a function of applied J value and various uncertainties of strain measurements. The strain uncertainty values in the fourth column from the left are absolute values ($\Delta\varepsilon_{11}^{2t}$) except for relative values ($\Delta\varepsilon_{11}^{2t}/\varepsilon_{11}^{2t}$) marked with #.

J (J/m^2)	P (N)	κ_2 (mm^{-1})	$\Delta\varepsilon_{11}^{2t}$ (-)	$\left(-\frac{\Delta H_2}{H_2}\right)^2$	$\left(\frac{\Delta\varepsilon_{11}^{2t}}{\varepsilon_{11}^{2t}}\right)^2$	$\left(\frac{\Delta J}{J}\right)$
10	128.15	27.1 x 10^{-6}	0.02$^{\#}$	0.16 x 10^{-3}	0.40 x 10^{-3}	0.03
10	128.15	27.1 x 10^{-6}	100 x 10^{-6}	0.16 x 10^{-3}	0.21	0.46
10	128.15	27.1 x 10^{-6}	300 x 10^{-6}	0.16 x 10^{-3}	1.9	1.39
10	128.15	27.1 x 10^{-6}	600 x 10^{-6}	0.16 x 10^{-3}	7.7	2.77
200	573.1	0.121 x 10^{-3}	0.02$^{\#}$	0.16 x 10^{-3}	0.40 x 10^{-3}	0.03
200	573.1	0.121 x 10^{-3}	100 x 10^{-6}	0.16 x 10^{-3}	11 x 10^{-3}	0.10
200	573.1	0.121 x 10^{-3}	300 x 10^{-6}	0.16 x 10^{-3}	96 x 10^{-3}	0.31
200	573.1	0.121 x 10^{-3}	600 x 10^{-6}	0.16 x 10^{-3}	0.38	0.62
1000	1281.5	0.271 x 10^{-3}	0.02$^{\#}$	0.16 x 10^{-3}	0.40 x 10^{-3}	0.03
1000	1281.5	0.271 x 10^{-3}	100 x 10^{-6}	0.16 x 10^{-3}	2.1 x 10^{-3}	0.05
1000	1281.5	0.271 x 10^{-3}	300 x 10^{-6}	0.16 x 10^{-3}	19 x 10^{-3}	0.14
1000	1281.5	0.271 x 10^{-3}	600 x 10^{-6}	0.16 x 10^{-3}	77 x 10^{-3}	0.28

From the tables we note that an increase in J increases both P and κ_2 (this is also expected from eq. (16)) and increases ε_{11}^{2t} (as expected from (25)). The higher strain means that the uncertainty contribution associated with strain measurement decreases. For example, from Table 3 it can be inferred that for J = 200 J/m^2, a value of H_2 = 8 mm gives a relative uncertainty of J of 22% (i.e., exceeding the acceptance criterion) for a strain uncertainty of 300 μstrain. But (still for H_2 = 8 mm) for the highest J value (1000 J/m^2) even the highest strain uncertainty (600 μstrain) would give a relative uncertainly of 20% on J, just within the acceptance criterion set here.

With other parameter fixed, an increase in H_2 leads to an increase in P and a decrease in κ_2, resulting in an increasing uncertainty in J for an uncertainty in strain resolution of 300 μstrain (corresponding to the expected uncertainty of DIC).

Insight can be gained by comparing the magnitude of the squared uncertainty terms (showed under the light green colors in Tables 1 to 4) associated with the various parameters. The contributions from P, ℓ_2 and B are in the order of 10^{-5} to 10^{-4} (Table 1). The squared uncertainty terms associated with H_2 and ε_{11}^{2t} are (in nearly all cases) larger. The squared uncertainty term from H_2 is in the range of approximately 10^{-4} to 0.01, decreasing with increasing H_2. The squared uncertainty contribution from ε_{11}^{2t} is in the order of magnitude of 10^{-4} to 1, increasing with increasing H_2. Comparing the tables, it is seen that in most cases, the uncertainty contribution from ε_{11}^{2t} is the largest contributor to the combined uncertainly of J. Optimization of specimen geometry could include reducing the term $(\Delta\varepsilon_{11}^{2t}/\varepsilon_{11}^{2t})^2$ to the same magnitude as the other terms.

5. Discussion

5.1. Limitation of the approach

Tables 2 to 4 show that for J = 10 J/m^2, a strain resolution of 300 μstrain gives an uncertainty of J that is larger than 20%. This suggests that DIC would not be suitable for measurement of strains for curvature for materials and interfaces having low fracture energy values. Measurement using strain gauges would most likely be needed.

In practice, it would be difficult to bond foil strain gauges to the bottom of Beam 1 and top of Beam 2 (the cracking plane). It is therefore highly desirable to be able to obtain the strain measurements from the frontal face of the beams using DIC. A broader sensitivity study could be made to determine the best specimen dimensions following the lines of the small example presented here.

The approach is not limited to the type of results given in Table 2 to 4. The formulas in Section 3.3 can for example be used to determine the strain resolution necessary to obtain a desired relative uncertainty (e.g., $\Delta J/J$ = 20% or maybe $\Delta J/J$ = 10%) for different levels of H_2 and J.

5.2. Practical measurement of ε_{11}^{2t} and ε_{11}^{2b}

As described earlier, for a beam segment loaded by an axial force and a bending moment, the strain component ε_{11} varies linearly across the beam height in accordance with (3) and (4), being independent of the x_1-position. Therefore, the averaging approach proposed by Wang and Tong [18] can be used for the present specimen remote from the fracture process zone. More precisely, the strain component ε_{11} could be averaged along the length for the same x_2-position (or as an example, y_2^*-position for Beam 2).

Furthermore, the fact that the strain varies linearly across the beam in accordance with (4), enables precise measurement of ε_{11}^{2t} and ε_{11}^{2b} (or κ_2 and ε_2^{0*}) as follows. First, as shown in figure 3a), the strain component ε_{11} is determined for many points along a line at a given x_2-position (the approach of Wang and Tong). These strain values are then averaged (see Fig. 3b). Likewise, the average value of ε_{11} is determined for points along another line at a smaller x_2-position. This can be done for several lines along the x_1-direction, creating a data set of $\varepsilon_{11} = \varepsilon_{11}(x_2)$. A straight line can be fitted to the $\varepsilon_{11}(x_2)$-data and the parameters κ_2 and ε_2^{0*} can be obtained by linear regression in accordance with (4). Such an approach might give a strain measurement accuracy better than the range of 300 - 600 μstrain obtained by Reu *et. al*. [19].

6. Conclusions

The J integral contributions for beams of beam-like specimens subjected to axial forces and bending moments can be calculated from measurement of applied loads and resulting deformation (strains and curvature) of three beams. No stiffness data are required. The approach eliminates the need to make additional tests to determine the tensile and bending stiffness~~es~~.

Such a testing approach is particularly useful for fracture mechanic characterisation of materials with unknown elastic properties, and specifically for analysis of substructure cut from old blades where the elastic properties and thickness of layers are not readily known.

The proposed approach of using digital image correlation for strain and curvature measurements for fracture mechanical characterisation by J may be associated with large uncertainties for materials and

interfaces that have a low fracture energy (here exemplified by a fracture energy of 10 J/m^2). But for materials and interfaces with higher fracture resistance (fracture energy in the order of 200 J/m^2 or higher), the proposed approach seems feasible.

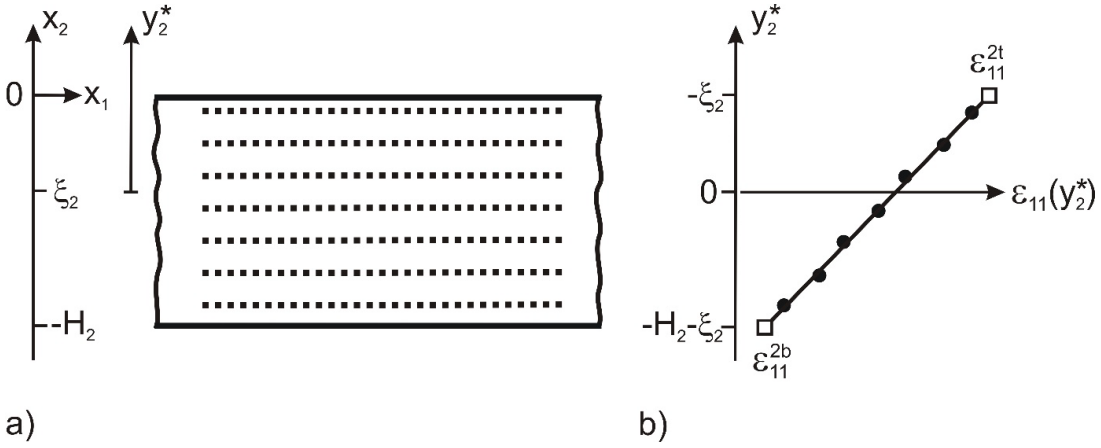

Figure 3. An approach for measurement of strain variation across a beam segment subjected to uniform extension and bending by the DIC technique. (a) measurement of strains of many points along several lines parallel to the beam (the x_1-directions), (b) for each line average points are anticipated to lie on a straight line, which allows extrapolation to identify ε_{11}^{2t} and ε_{11}^{2b}.

Acknowledgements
This works was made as a part of the ReLife project ("Methodology for assessment of remaining life time of wind turbine blades based on damage state") funded by the Energy Technology Development and Demonstration Programme (EUDP) under the Danish Energy Agency (grant no. 64019-0543).

References

[1] ASTM D5528-01 (2001); "Standard test for Mode I interlaminar fracture toughness of unidirectional fiber-reinforced polymer matrix composites", American Society for Testing and Materials, West Conshohocken, Pennsylvania.
[2] ASTM D6671/D6671M-22 (2022), "Standard Test Method for Mixed Mode I-Mode II Interlaminar Fracture Toughness of Unidirectional Fiber Reinforced Polymer Matrix Composites", American Society for Testing and Materials, West Conshohocken, Pennsylvania.
[3] Sørensen B F, Jørgensen K, Jacobsen T K and Østergaard R C 2006 *Int. J. Fract.* **141** 159
[4] Sørensen B F and Jacobsen T K 2009 *Comp. Sci. Techn.* **69** 445
[5] Paris A J and Paris P C 1988 *Int. J. Fracture* **38** R19
[6] Olsson P and Stigh U 1989 *Int. J. Fracture* **41** R71
[7] Rask M and Sørensen B F 2012 *Engr. Fracture Mechn.* **96** 37
[8] Sarrado C, Turon A, Renart J and Costa J 2015 *Comp. Sci. Techn.* **117** 85
[9] Toftegaard H L and Sørensen B F 2019 *Engr. Fracture Mechn.* **217** 106500
[10] Sutton M A, Cheng M, Peters W H, Chao Y J and McNeill S R 1986 *Image Vis. Comput.* **4** 143
[11] Rice J R 1968 *J. Appl. Mech*. **35** 379
[12] Beer F P and Russell Johnston E Jr 1992 *Mechanics of Materials* (London: McGraw-Hill), 2 edit.
[13] Taylor J R 1982 *An introduction to error analysis. The study of uncertainties in physical measurements* (Sausalito, University Science Books, second edition)
[14] Carlsson L A, Adams D F and Byron Pipes R 2014, *Experimental characterisation of advanced composite materials* (Boca Raton: CRC Press, Taylor & Francis Group), 4th ed., Appendix C.

[15] Hannah R L and Reed S E 1992 *Strain gage users' handbook* (Dordrecht: Elsevier Science Publishers) p. 137
[16] Dally J W, Riley W F and McConnell K G 1984 *Instrumentation for engineering measurements*, John Wiley and Sons p. 193, p. 205
[17] Smith B W, Li X and Tong W 1998 *Experimental Techniques* **22** 19
[18] Wang Y G and Tong W 2013 *Optics and Lasers in Engineering* **51** 30
[19] Reu P L, Toussaint E, Jones E, Bruck H A, Iadicola M, Balcaen R, Turner D Z, Siebert T, Lava P and Simonsen M 2018 *Experimental Mechanics* **58** 1067
[20] Instron 2527 Series Bi-axial Dynacell Load Cells, https://www.instron.com/en/products/testing-accessories/load-cells/dynamic-fatigue.
[21] Sørensen B F and Jacobsen T K 1998, *Comp. A.* **29A** 1443